postprint Langmans, J., Klein, R., Roels, S. (2012). Hygrothermal risks of using exterior air barrier systems for highly insulated light weight walls: A laboratory investigation. Building and Environment, 56 (10), 192-202.

Hygrothermal risks of using exterior air barrier systems for highly insulated light weight walls: a laboratory investigation

Jelle Langmans[a,*], Ralf Klein[b], Staf Roels[a]

[a] *Department of Civil Engineering, Building Physics Section, University of Leuven*
Kasteelpark Arenberg 40 - bus 02447, BE-3001 Heverlee, Belgium
[b] *Sustainable Building Research Group, Departement of Industrial Engineering, Catholic University College Sint-Lieven*
G. Desmetstraat 1, BE-9000 Ghent, Belgium

** Corresponding author. Tel: +32 16 321348; fax: + 32 16 32 19 80.*
E-mail address: jelle.langmans@bwk.kuleuven.be (J. Langmans)

Abstract

The current paper presents the results of a detailed laboratory experiment to study the hygrothermal behaviour of vertical light weight walls with an exterior air barrier. Four independent test walls (each 2.3m by 0.5m) are placed between a newly developed hot and cold box, operating at controlled temperatures, humidities and air pressures. All four walls are insulated with 30 cm of standard mineral wool to which OSB is applied as interior vapour retarder. The test walls differ from each other by the physical properties of applied exterior air barrier; airtightness, moisture buffer capacity, vapour permeability and thermal resistance. An additional objective of the current investigation is to generate validation data for numerical HAM models. As a consequence, great care was given to create precise two dimensional conditions and to minimize air leakages.

The results reveal that using an exterior air barrier instead of traditional interior one, may increase the moisture load as a result of buoyancy driven convection. This leads to an increased risk for mold growth and interstitial condensation against the upper position of the exterior sheathing in winter conditions.

Keywords: Hygrothermal analysis, hotbox-coldbox, exterior air barrier, natural convection, laboratory

1. Introduction

A sound global building airtightness is one of the prerequisites to achieve energy efficient buildings [1]. As a consequence, several European member states increased their airtightness requirements. Moreover, labels to certify standardised low energy buildings, requiring very high airtightness standards, are becoming more and more popular in Europe. For example the 'Passive House'-standard [2] and the 'Minergy-P'-standard [3] explicitly require a building airtightness of 0.6 air changes per hour (ACH) at 50 Pa. Apart from improving energy efficiency, the second major motivation for creating airtight building envelopes is moisture control. Interstitial condensation in building enclosures is primarily the result of forced air exfiltration in winter conditions [4, 5]. Condensation quantities related to exfiltration are two to three orders of magnitude higher than those transported by vapour diffusion [6,7]

For timber frame construction an airtight building envelope is traditionally realised by an interior 'air barrier system', by sealing all the joints and intersections in the interior sheathing. In cold and moderate climates, such as North-West European areas, this air barrier function is often combined with that of the 'vapour retarder' [8]. To protect the insulation layer from unwanted infiltration of outside cold air by natural or forced

convection a ‘wind barrier’ is provided at the outside of the insulation [9]. In addition, this exterior layer serves as drainage plane to prevent water infiltration into the structure. The performance criteria for wind barrier systems regarding air permeance are less severe than for air barriers [8]. Therefore, the sealed joints in the wind barrier are usually limited to the critical joints regarding water infiltration [10].

Achieving the above mentioned high standards regarding global building airtightness with an interior barrier is very labour-intensive. In installing an interior barrier a high number of difficult intersections, such as the connection between the intermediate floor and the outer walls, and perforations for electrical and plumbing services have to be sealed [11-14]. As a result, building industry is looking for cost-effective techniques to meet the severe airtightness requirements. One of the possibilities is to move the interior air barrier to the outside of the building envelope where fewer joints are present. Recent studies show the advantage of improving the airtightness of the wind barrier, so, it will serve as an exterior air barrier system. *In-situ* measurements combined with laboratory tests show how minor modifications can significantly improve the air permeance of the wind barrier layer [10]. This study demonstrated that with good workmanship and appropriate materials, an airtightness level lower than 1 ACH at 50 Pa can be reached with only the wind barrier. Mainly in Norway this technique is increasingly applied and successful cases are documented in the literature [15-18]. As a result it is becoming common practise to measure the global building airtightness twice in Norway; during the windtight stage and after the building is finished.

However, when improving the wind barrier to such levels it becomes impossible to control the continuity of the interior air barrier with pressurisation tests because only the air resistance of the global building envelope is measured. This means that situations in which the exterior wind barrier is far more airtight than the inner air barrier are very likely to occur. In this case the exterior sheathing will act as a wind and air barrier and the inner sheathing acts only as a vapour barrier/retarder. In this way the most critical moisture load, being forced air exfiltration, is still excluded by the exterior air barrier. But, given the non-continuous interior sheathing, other transport mechanisms such as internal natural convection might be introduced. Figure 1 gives an overview of the different buoyancy driven air flow patterns depending on the air permeance of the interior and exterior sheathing of a light weight wall. For these configurations the influence of natural convection on the thermal performance is well documented in the literature [19-21]. In summary, these studies conclude that the impact of natural convection on the thermal performance is limited when at least one of the adjacent layers is airtight (Figure 1a, 1b and 1c), air gaps along the interface between the sheathing and insulation are avoided and sufficiently dense insulation materials (>20-30 kg/m³) are applied .

On the contrary, the moisture redistribution caused by this internal natural convection process is scarcely investigated for building components. Most studies focus on the effect of forced air exfiltration problems [3,4,5,22,23]. When it comes to natural convection, only the first configuration of Figure 1 (airtight layer on both side of the insulation) is studied [24, 25]. The results of Riesner [25] give clear evidence of a redistributed moisture field caused by natural convection depending on the air permeability of the insulation layer. However, the formulated recommendations regarding the insulation are valid only for the configuration with both the interior and exterior airtight [26]. In case of an air open interior sheathing (Figure 1b) this effect might be more dominant since inside air with a higher absolute humidity can enter the insulation at the upper position. Consequently the question arises to which level the risk for interstitial condensation or mould growth against the airtight exterior sheathing increases.

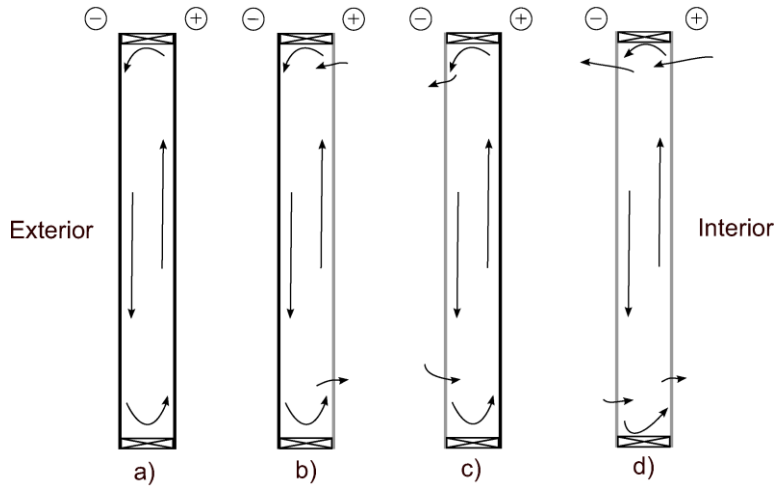

Figure 1. Buoyancy driven air flow in a light weight wall: a) airtight interior and exterior sheathing, b) air open interior sheathing, c) air open exterior sheathing, d) air open interior and exterior sheathing

The current paper presents the results of a comprehensive laboratory investigation in which the hygrothermal response of light weight walls with an exterior air barrier is studied. Main objective of the paper is to acquire insights in the hygrothermal risk of exterior air barriers and collect at the same time a detailed validation set for numerical Heat, Air and Moisture models.

Four highly insulated timber frame walls enclosed between two climate chambers to simulate winter conditions in a temperate climate have been analysed. The test walls are based on the configuration currently used in Belgian timber framed Passive houses using Oriented Strand Board (OSB) as interior sheathing and insulated with 30 cm of insulation. The walls differ from each other by the physical properties of the applied exterior air barrier: the airtightness, moisture buffer capacity, vapour permeability and thermal resistance of the air barriers

vary. The investigation is performed in five consecutive stages with increasing rates of air transport in the test walls.

2. Experimental Method

2.1. Hot box/ cold box equipment

A new vertical calibrated hot box/ cold box was constructed at the Laboratory of Building Physics, University of Leuven to investigate the hygrothermal performances of highly insulated building components. The test setup consists of three major parts; a test frame to install the studied building component enclosed between two climate chambers to simulate indoor and outdoor conditions (Figure 2). To reduce the heat losses through the calibrated hot box to a very minimum, the hot box is insulated with 60 cm polyurethane (R=30 Km^2/W). The warm climate chamber has a cubic inner volume with sides of 2.4 m and is completely separated from the laboratory conditions without any thermal bridge (Figure 3). The test frame, which was constructed in the same way, has a measuring area of 2.4 m by 2.4 m and a depth of 0.6 m. The cold box on the other hand is insulated with only 0.1 m polyurethane boards. The clamping system to connect the three parts consists of a screw system with 7 bars distributed over the total height of each side of the test setup (Figure 2). In combination with compressible closed cell polyurethane foam with a thickness of 2 cm, this system provides an airtight and insulated connection between the different parts.

Figure 2. Picture of the vertical hot box – cold box

A controlled IR-bulb in the middle of the warm chamber creates the desired temperature conditions. Figure 3 (vertical section) shows how the IR-bulb is covered with a reflective foil to avoid direct long wave radiation towards the test component. The cold chamber is provided with a liquid-to-air heater exchanger accompanied

with a fan system to control and distribute the temperature. The fan system, which can simulate wind effects, allows a steady state air flow along the test wall with velocities between 0.5 – 10 m/s. The humidity in both the warm and cold chamber is conditioned with free evaporation of salt solutions. To create a total air pressure difference across the test section, a small ventilator is installed at the back of the warm chamber.

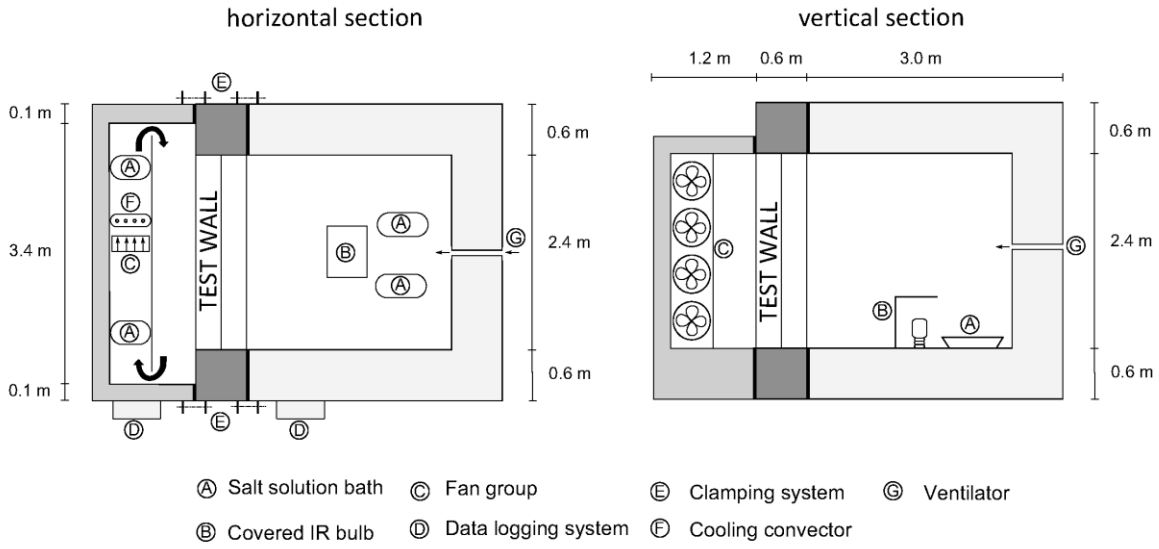

Figure 3. Vertical hot box – cold box experiment: horizontal and vertical cross section.

2.2. Wall configurations

To investigate the hygrothermal consequences of exterior air barrier systems in timber frame construction, four highly insulated walls (each 2.3m by 0.5m) were tested. The test walls are designed consistent with the current practice for timber frame Passive houses in Belgium. All four walls are insulated with 30 cm of standard mineral wool to which OSB is applied as interior vapour retarder. The test walls differ from each other by the physical properties of the applied exterior air barrier; airtightness, moisture buffer capacity, vapour permeability and thermal resistance. Both the exterior sheathing of the first test wall (herein referred to as REFERENCE) and the second test wall (referred to as FIBREBOARD 1) consist of bituminous impregnated soft fibre board with an exterior top layer which increases its airtightness. For the third test wall (FIBREBOARD 2) a similar bituminous impregnated soft fibreboard but without the exterior top layer is applied. This means that the first three test walls are provided with a hygroscopic exterior sheathing. The fourth wall (FOIL), on the other hand, is executed with a spunbonded foil at the outside. The applied foil is extremely airtight but has no moisture buffer capacity. Behind the exterior air barrier an air cavity of 5 cm is left, which is closed with a fly screen. The aim of this screen is to provide an air and vapour open layer which prevents vortices introduced by the air movement of the ventilator in the cold box. This is important in achieving equal air pressure differences across the different wall sections. The

configuration of the test walls studied is shown in Figure 4 and the most important material properties are summarised in section 2.5. The walls are separated with a polyurethane board (5cm) in between two wood fibreboards (1.8 cm) which are covered with an airtight and watertight paint to prevent any significant heat or mass exchange between the test walls.

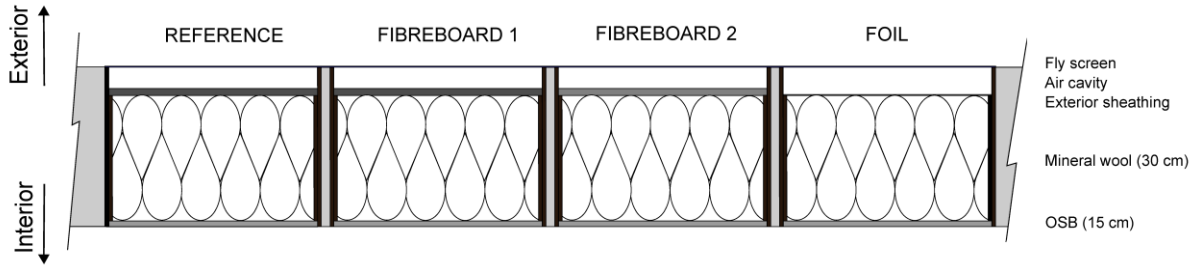

Figure 4. Wall configurations studied

2.3. Boundary conditions and test sequence

The experiment, which lasted about four months, was subdivided in five main consecutive measuring steps. In the first four steps the test walls were exposed to typical winter conditions with increasing rates of natural and forced air convection.

During the first step, both the interior and exterior sheathing are airtight. In the second step, gaps are introduced in the interior barrier of all walls except for the REFERENCE section. The gaps correspond to slots of 1 cm at 20 cm from the top and bottom of the OSB and extend the full width of each test wall to maintain the two dimensional situation. In step 3 and 4 the hotbox was pressurised.

Finally, in the last step the conditions in the cold box were adapted to create drying conditions inside the walls. Table 1 summarises the boundary conditions in both the warm and cold chamber. The first four climate conditions represent an averaged typical winter month in a temperate climate, such as Belgium. The fifth step, on the other hand, corresponds to arbitrary drying conditions. In this table the boundary conditions correspond to the median, based on 10-minute data for each measuring step. To illustrate the variations on the boundary conditions, also the 5 and 95 percentiles based on 10-minute data are given in grey in Table 1. The percentiles which deviate by more than 10% from the corresponding median are underlined. The origins of these deviations are all temporary disturbances in transition to a next step. For example at the beginning of step 3, the inflated air from the laboratory was not yet pre-conditioned, resulting in dryer conditions in the hotbox. Or at the beginning of step 5, the ventilator in the hot box was still working, influencing the pressure difference across the wall and

thus the temperature and humidity in the hot box. Overall it may be concluded that the boundary conditions are very stable during the measurements.

	Days	T_{HB} (°C)			$P_{v,HB}$ (Pa)			T_{CB} (°C)			$P_{v,CB}$ (Pa)			P_a (Pa)		
1	35	20.0	20.1	20.1	1169	1181	1191	2.9	3.0	3.0	634	653	656	1.7	1.9	2.0
2	28	20.0	20.0	20.1	1168	1178	1205	3.1	3.2	3.7	676	680	698	0.6	0.8	1.4
3	24	20.0	20.1	20.1	968	1243	1333	3.1	3.2	3.2	678	685	689	5.7	5.8	6.0
4	11	20.1	20.1	20.2	1232	1249	1344	3.1	3.2	3.3	689	691	696	10.4	10.7	10.9
5	32	21.3	25.0	25.4	1384	1688	1723	22.4	22.6	22.6	1964	1997	2149	1.1	1.7	5.3

Table 1. Boundary condition in hotbox (HB) and coldbox (CB) during the consecutive measuring steps (5 and 95 percentiles in grey)

2.4. Sensor positioning and accuracy

To fully register the physical phenomena, a comprehensive data logging system was designed. Each test wall is provided with 18 thermocouples, 15 relative humidity sensors, 3 heat flux sensors and 1 pressure gauge sensor, covering the most important positions of the wall. The sensors are distributed in three rows: at 20 cm from the bottom, mid height, and 20 cm from the top and are placed at 15 cm from the left side. Figures 5 depicts an overview of the sensor positions as placed within each wall. The insulation blankets were installed in two layers (15cm-15cm) in order to attach temperature and relative humidity sensors in between. The blankets were carefully installed by pushing them with a rigid board into the cavity. In this way the correct position of the blankets, and thus the sensors, could be guaranteed.

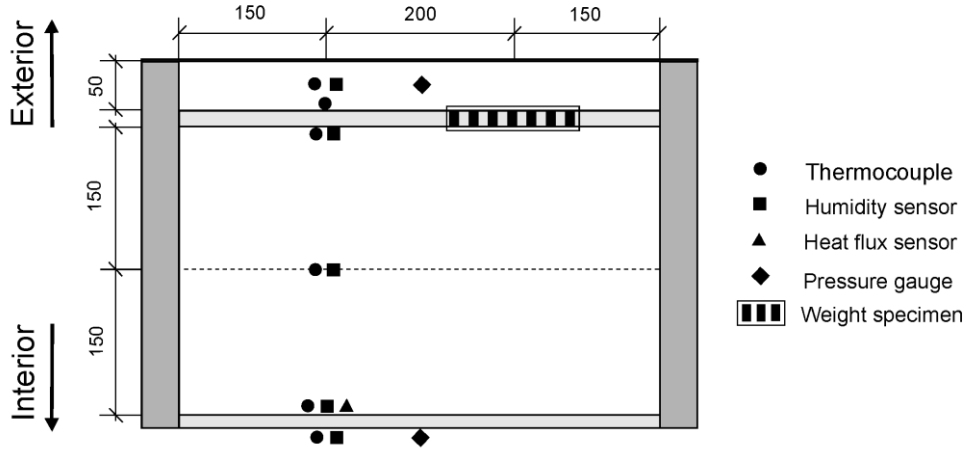

Figure 5. Sensor positioning within each wall section (distances in mm)

Besides the continuous logging system, the wind barrier layer was constructed in such a way that each part of the wall contained three removable specimens (18cm by 18cm). The specimens, placed at 15 cm from the right side, are used to quantify the moisture evolution of the fibreboard by weighing the specimens at regular time intervals.

Since the weight specimens were created in the exterior air barrier, it is of great importance to preserve the airtightness of this layer. Therefore, the perimeter of the specimens was step-like cut out of the fibreboard (Figure 6a). A very thin plexiglas layer was attached around the perimeter of the specimens and the board. In this way the joint could be taped in between the measuring steps without destructing the fibreboard (Figure 6b). To check the quality of the sealing, the airtightness of a board with a specimen was measured in the laboratory. The air permeability of the fibreboard with sealed specimen showed to be less than 5% more than the fibreboard only.

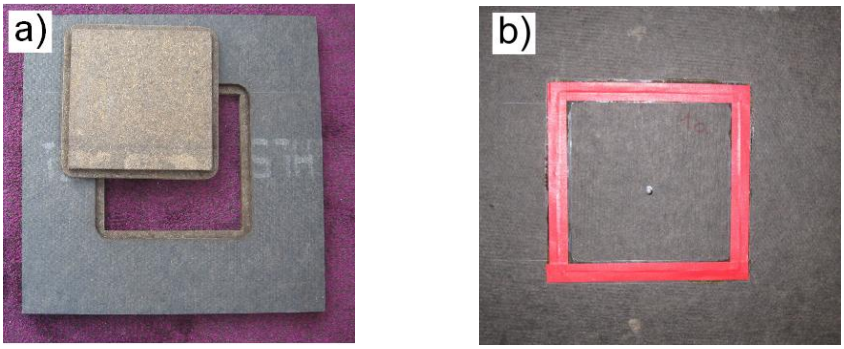

Figure 6. Weight specimen in hygroscopic exterior sheathing

To increase the reliability of the measurements the complete set of thermocouples, humidity sensors and heat flux sensors was calibrated in the laboratory. With a sensor specific calibration the accuracy of reading could be increased compared to the global sensor accuracy given by the manufacturer. In this way it is possible to compensate for errors such as the cold junction temperature and the position of the connection. The thermocouples and relative humidity sensors were calibrated with an optical dew point transmitter with an accuracy of +/-0.1 °C on the global temperature and +/-0.2°C on the dew point temperature. The thermocouples were calibrated at four temperatures (1, 10, 20 and 25 °C) and the humidity sensors at three humidities (30, 80 and 99% RH). The heat flux sensors, on the other hand, were calibrated in a heat flow apparatus as described in the standard guidelines [27]. Table 2 summarizes the applied sensors with the corresponding accuracy levels and measuring range.

Sensor	Manufacturer	Type/Model	Accuracy	Range
Thermocouple	Thermo Electric	Type T (class 1)	± 0.2 °C	-20/60 °C
RH-sensor	Honeywell	HIH-4000/21	± 2 %	0/100%
Pressure gauge	Halstrup Walcher	P 26	± 0.6 Pa	± 50 Pa
Heat flux transducers	Phymeas	Model 7	± 6% of reading	± 100 W/m²

Table 2. Accuracy and measuring range of applied sensors

2.5. Material properties

This section gives an overview of the hygrothermal properties of the applied materials in the experiment. As mentioned above only the exterior air barrier of the four test walls differs. Three different air barrier materials were carefully selected to compare a maximum number of different phenomena. The parameters investigated are the thermal resistance (FIBREBOARD 1 = FIBREBOARD 2 > FOIL), hygroscopic buffer capacity (FIBREBOARD 1 = FIBREBOARD 2 > FOIL), air permeance (FIBREBOARD 2 > FIBREBOARD 1 > FOIL) and vapour permeance (FIBREBOARD 1 < FIBREBOARD 2 < FOIL) of the different exterior sheathing materials.

Upper limits for the air permeance of air barrier systems, including joints and penetrations, are discussed in [28]. These air leakage rates, given as function of the vapour permeance of the outermost layer, were established through a computer modelling program (TCCCD [29]) carried out by IRC researchers in conjunction with the Technical Research Center (VTT) in Finland (Table 3). In Table 3 and the remainder of this work, the vapour resistance is expressed as the vapour diffusion-equivalent air layer thickness, s_d (m).

Vapour resistance (m) of outermost un-insulated (non-vented layer of the wall assembly)	**Maximum permissible air leakage rate (l/s.m²) at 75 Pa**
12.5 < s_d-value < 3.1	0.05
3.1 < s_d-value < 1.1	0.1
1.1 < s_d-value <0.23	0.15
s_d-value <0.23	0.2

Table 3. Maximum permissible air leakage rate – air barrier system [28]

All three exterior air barrier materials tested have a lower s_d-value than 0.23 m, so, the air leakage rate should not exceed 0.2 l/(s.m²) at 75 Pa according to [28]. In this respect one exterior sheathing material was chosen to exceed this threshold value; the air leakage through Fibreboard 2 at 75 Pa corresponds to 2.3 l/s.m². The other two materials, Fibreboard 1 (0.1 l/s.m²) and Foil (<0.02 1/s.m²) satisfy this standard.

2.5.1. Heat transfer properties

Table 5 gives an overview of the heat transfer properties of the used materials. The heat conductivity of the materials was measured at the laboratory according to [27]. The thermal conductivity λ (W/m/K) was measured as function of the temperature and fitted with the following linear relation:

$$\lambda = \lambda_0 + \theta.\lambda_\theta \quad (1)$$

where λ_0 (W/m/K) corresponds to the thermal conductivity at 0°C, θ expresses the temperature (°C) and λ_θ describes the temperature dependency. The heat capacity c_p was collected either from product sheets or the literature [30].

2.5.2. Air transfer properties

All the air permeability measurements were performed with the test-setup described in [14]. The permeability of the mineral wool was measured both perpendicular $K_\perp$ and parallel $K_\parallel$ to the fibres on specimens of 0.2x0.2x0.2 m^3. The results are compared with values from the literature in Table 4. The permeability values are in good agreement with the values from the literature. Only the permeability perpendicular to the fibres is slightly lower than values from the literature. However, in addition Table 4 gives the minimum and maximum measured values between brackets from which can be concluded that there is a large variation on the permeability parallel to the fibre. It was noticed that depending on how secure the specimen was installed in the test rig, large differences were measured. Consequently it is very difficult to determine the exact air permeability of the mineral wool as installed in the test walls.

	ρ (kg/m³)	**$K_\perp$ (10^{-9} m²)**	**$K_\parallel$ (10^{-9} m²)**
Økland [24]	18.3	1.7	3.7
Kronvall [31]	20	2.2	4.1
present study	21.3	1.3 (1.1 -1.5)	3.8 (2.4 - 5.7)

Table 4. Air permeability of mineral wool (minimum/maximum between brackets)

The air permeability values of the sheathing materials were also measured in the laboratory and are summarized in Table 5. So far only the air permeability values of porous materials are discussed. Air transport through a porous medium can be described by Darcy law, and corresponds to a constant permeability. However, when it comes to air transport through air leakage paths, such as the horizontal slots in the OSB layer, the air resistance depends on the pressure difference. Mostly this is described as a power law function. Figure 7 gives the measured air flow through a 1cm slot in an OSB specimen.

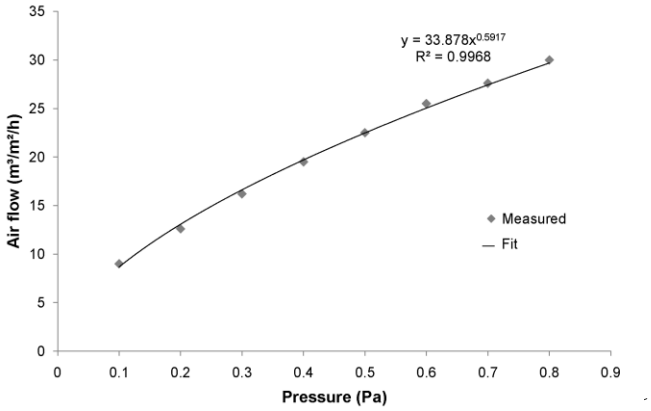

Figure 7. Air leakage through gap of 1 cm in OSB

2.5.3. Hygric properties

The moisture capacity of the building components is measured by determining the hygroscopic sorption curves. The results, which are fitted with equation 2, are shown in Figure 8a.

$$u = v(1 + (m.\ln(\phi))^n)^{\frac{1-n}{n}} \quad (2)$$

where u is referring to the moisture content (kg/kg), ϕ is the relative humidity (%) and v, m and n are fitting parameters. Also water vapour transmission properties of the applied materials were measured at 23 °C according to [32] . The results, which are fitted with equation 3, are shown in Figure 8b.

$$s_d = \frac{1}{a+b.e^{c\phi}} \quad (3)$$

in which s_d represents the water vapour diffusion-equivalent air layer thickness, ϕ is the relative humidity (%) and a, b and c are fitting parameters.

Liquid water transport in the interior sheathing and mineral wool insulation is unlikely to occur. Therefore only the water absorption coefficients of the exterior fibreboard sheathings were measured according to [33]. The results reveal that these materials are non-capillary. The moisture increase during the absorption experiment has the same order of magnitude as the hygroscopic loading of the material. Additional contact angle measurements confirmed the hydrophobic behaviour of these materials. In summary, we conclude that Fibreboard 1 and 2 are strongly hygroscopic, moisture buffering and vapour permeable, but non-capillary.

	Fibreboard 1	Fibreboard 2	Foil	OSB	Mineral Wool
d (mm)	18	18	0.2	15	300
ρ (kg/m³)	285	274	-	630	21.3
c_p *(J/(kgK))*	2068	2068	-	1880	840
λ_0 *(W/m/K)*	0.045	0.047	-	0.1	0.031
λ_Θ	0.0001	0.0001	-	0.0002	0.0001
$K_\perp$ *(m²)*	4.65E-14	1.37E-12	*airtight*	8.20E-15	1.30E-09
$K_\parallel$ *(m²)*	-	-	-	-	3.80E-09

Table 5. Hygrothermal material properties

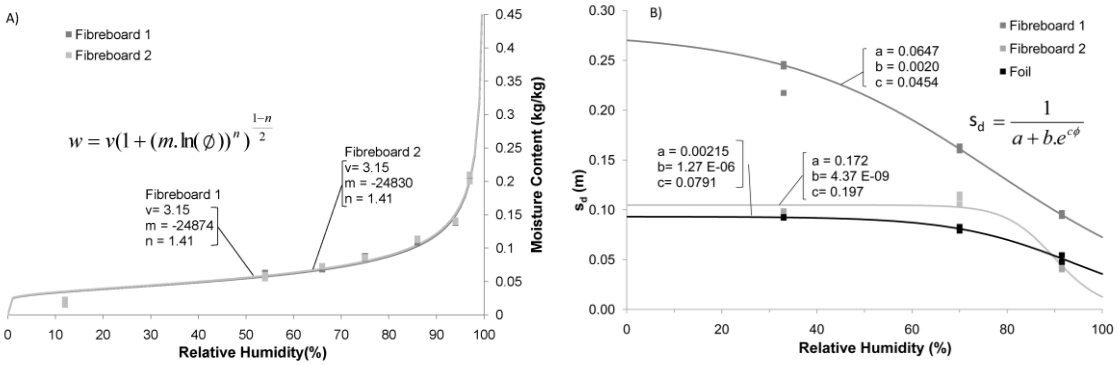

Figure 8. Sorption isotherm (a) and vapour diffusion resistance (b) of the different exterior sheathing materials as function of relative humidity.

3. Test results

3.1. Thermal response

As a first step in analysing the results we focus on the thermal distribution in the test walls. Figure 9 shows the dimensionless temperature profiles of the four walls at the top and bottom row for measuring stage 1, 2 and 4. This corresponds to the situations where (1) the interior OSB sheathing is intact, (2) top and bottom gaps in the interior sheathing are introduced and (3) a pressure differential of 10 Pa across the test wall is realised.

This figure clearly shows that during the first step (blue triangles) the temperature distribution for all four walls bends upwards at the top (filled markers) and downwards at the bottom (open markers) which indicated the existence of natural convection within the walls. This was studied more in depth with additional numerical simulations in [34]. This study, which simulates the heat transfer through similar test walls as described in the current article, concludes that the existence of very small vertical gaps between the mineral wool and the sheathing material combined with the (local) increase of the air permeability of the installed mineral wool has a great influence on the magnitude of natural convection inside the walls. Similar results of the influence of workmanship on the performance of mineral wool insulation were found in [19-20]. However, as shown in [34]

the impact on the overall heat flux through the walls is still negligible when the gaps are less than 3 mm, which is certainly the case for the configuration studied in the present article.

During the second measuring step (red squares) this effect increases as a result of the introduction of the gaps in the interior sheathing. In addition, it is also noticed that the temperature profile for the least airtight wall (FIBREBOARD 2) bends also upwards at the bottom row. This means that the exterior sheathing is even so air permeable that as a result of the 1.9 Pa pressure differential across this wall (introduced by the ventilators in the cold chamber) forced exfiltration already dominates the air flow in this section. When finally a pressure difference of 10 Pa (green dots) is realised in the fourth step this effect becomes of course much more pronounced in FIBREBOARD 2. Also for FIBREBOARD 1 this effect is (to a minor degree) observed. For the moist airtight wall (FOIL) this remains negligible.

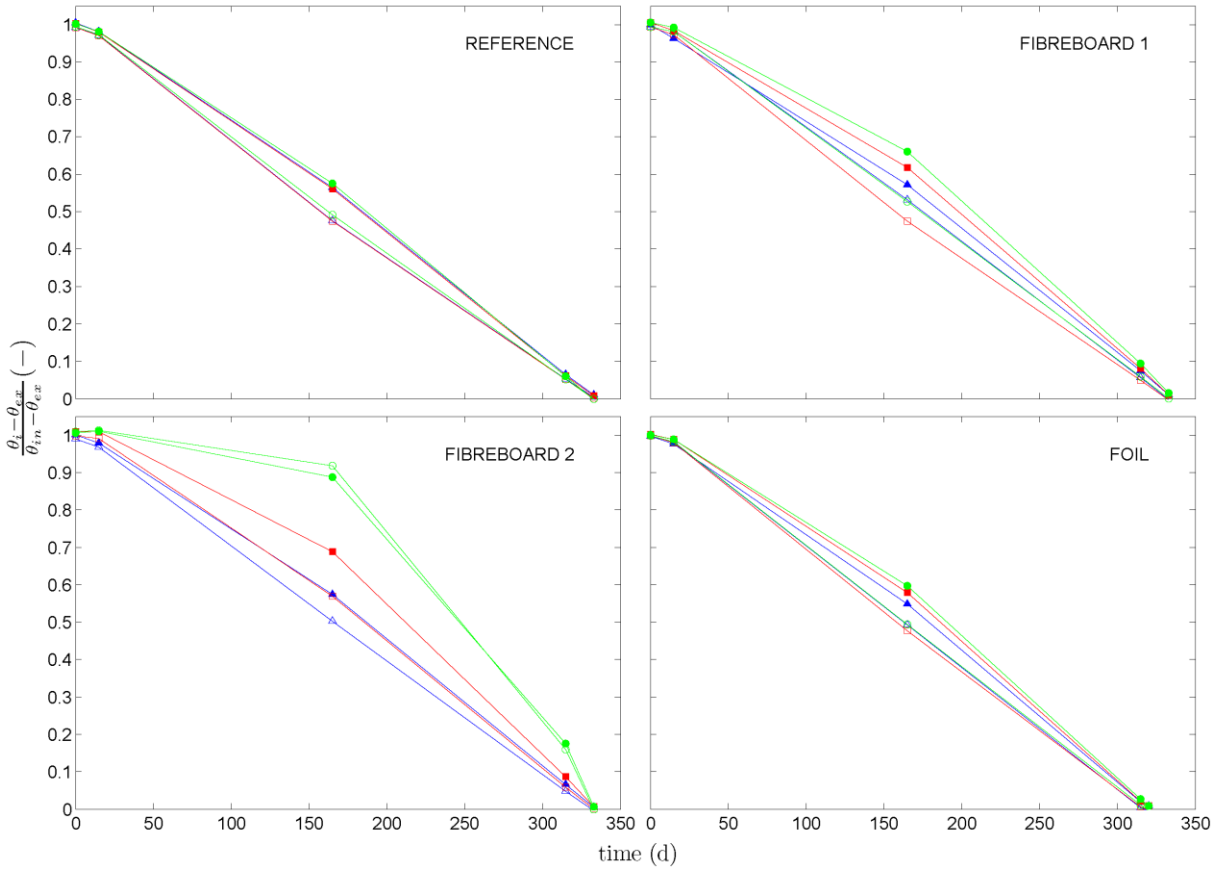

Figure 9. Dimensionless temperature profile of four test walls at top row (filled markers) and bottom row (open markers) during measuring step 1 (blue triangle), step 2 (red square) and step 4 (green dot).

3.2. Hygrothermal response

The main interest lies upon to the hygric behaviour of the system. Since the relative humidity, and thus moisture contents are function of the temperature, the current section focuses in a first step on the vapour pressure. This

quantity, independent from the temperature, is derived from the measured temperatures and relative humidity according to:

$$P_v = \phi \cdot \exp\left(65.8 - \frac{7066.3}{T} - 5.98 \cdot \ln(T)\right) \quad (4)$$

where P_v (Pa) corresponds to the vapour pressure, ϕ to the relative humidity (%) and T (K) to the temperature.

The notation of section 3.1 is used to present the dimensionless vapour pressure profiles across the test walls in Figure 10.

During the first step all four walls show a similar vapour pressure profile; a steep drop behind the vapour retarder (OSB) followed by a slight decrease towards the outer side. Only for FIBREBOARD 1 the vapour pressure at the top row is somewhat deviating from the expected values. At this row the vapour pressure is slightly higher than in the other walls. This can not be the result of air exfiltration since this should be noticed in the temperature distribution as well. A more plausible explanation might be found in a local deviation of the vapour resistance in the interior/exterior sheathing material or the sealed gap.

In the subsequent step, when the gaps in the interior sheathing are opened, the influence of natural convection on the moisture load becomes very pronounced. For all walls with interior gaps the vapour pressure at the top row increases while the vapour pressure at the bottom row remains almost the same. Only for FIBREBOARD 2 also the vapour pressure at the bottom row increases since forced exfiltration is then already dominant as a result of the high air permeance of the exterior sheathing as discussed in the section 3.1.

When a pressure difference of 10 Pa is realised the vapour pressure profiles confirms the observation of the temperature profiles. For FIBREBOARD 1 a slight increase in vapour pressure is noticed as a result of forced exfiltration while this effect is much stronger in FIBREBOARD 2. For the wall with the exterior foil this influence is hardly noticed.

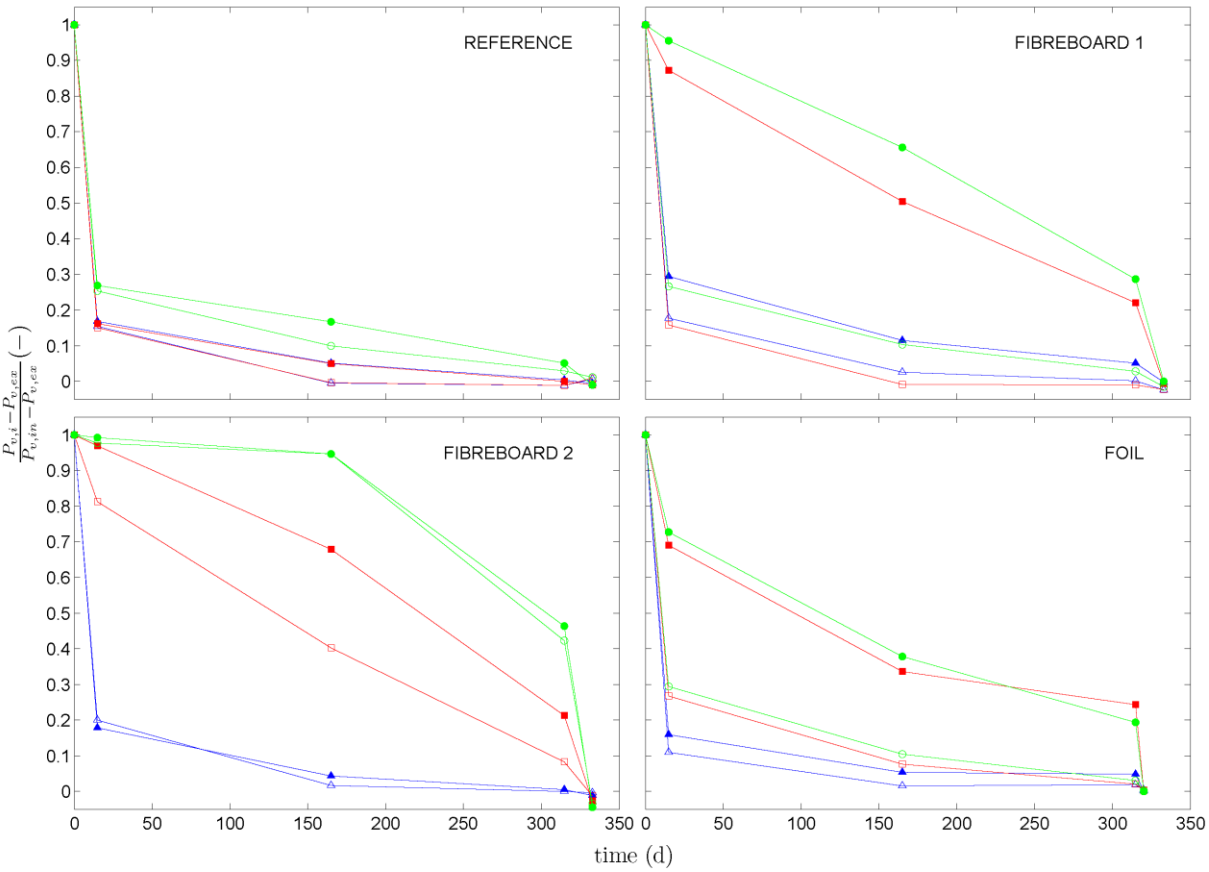

Figure 10. Dimensionless vapour pressure profile of four test walls at top row (filled markers) and bottom row (open markers) during measuring step 1 (blue triangle), step 2 (red square) and step 4 (green dot).

In addition to the dimensionless vapour pressure profiles Figure 11 shows the evolution of the relative humidity at the interface of the exterior air barrier and insulation for the three heights. This figure also plots the relative humidity in the cold (blue surface) and warm (red surface) chamber.

During the first step, when the interior gaps were still sealed, the relative humidity of the walls with an exterior fibreboard sheathing are in the same range. As a result of the moisture buffer capacity it takes time before the relative humidity reaches a quasi-equilibrium state. Real equilibrium is not obtained since the relative humidity in the cold chamber slightly increases during the measurement (blue surface). The wall with an exterior foil on the other hand, reaches this state almost immediately after starting the experiment. Additionally it is noticed that the relative humidity of the wall is 6 to 9% higher compared to the reference wall. Nevertheless the foil has a higher vapour permeance, the lack of thermal resistance causes lower temperatures at this position compared to the other walls. Consequently this results in a lower saturation pressure and thus higher relative humidities.

In the next step, after opening the gaps at the interior OSB-layer, the upper relative humidity against the foil peaks towards condensation conditions. The same happens for the FIBREBOARD 1 and FIBREBOARD 2, however, with a slower progress as result of the moisture buffer of the fibreboards. Contrary to FIBREBOARD 1 and FOIL, also the relative humidity at the middle and bottom position of FIBREBOARD 2 increases during the

second step. As explained in the previous paragraph this is the result of the small pressure differential created by the ventilator in the cold box combined with the high air permeance of this fibreboard.

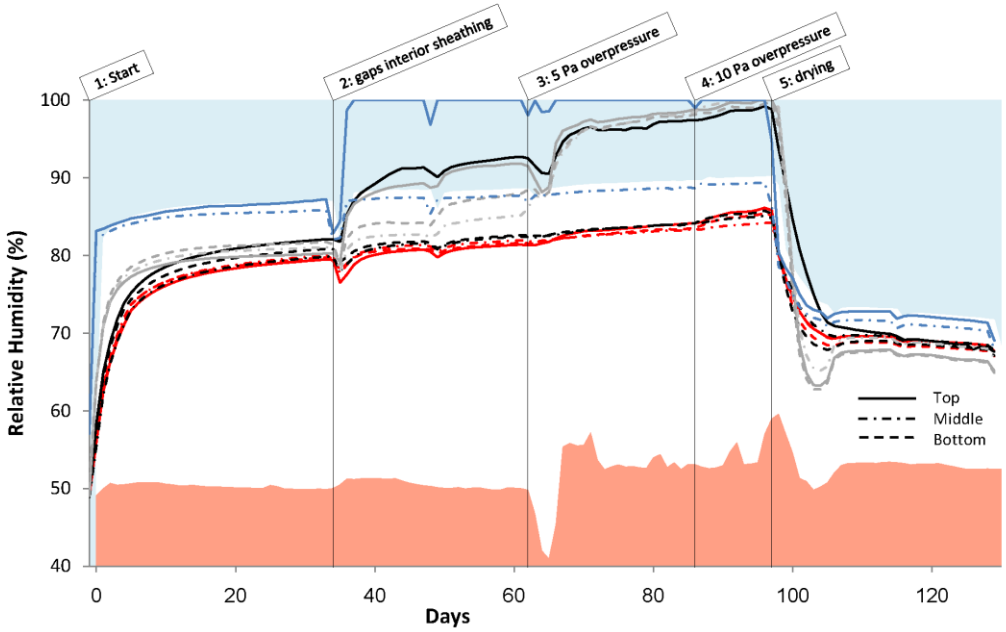

Figure 11. Relative humidity (%) at the interface insulation-exterior air barrier for REFERENCE (red), FIBREBOARD 1 (black), FIBREBOARD 2 (grey) and FOIL (blue)

In the next two step (3 and 4), the same evolution continues. Driven by forced convection the relative humidity at the middle and bottom position of FIBREBOARD 2 converges towards the upper one. At the end of step 4 the relative humidity levels at the upper position of FIBREBOARD 1 and FOIL and at all three heights of FIBREBOARD 2 correspond to nearly the same high values. Figure 8 shows how such high relative humidities (>95%) correspond to a steep peak in the hygroscopic curve. At these high relative humidity levels the hygroscopic curve becomes very uncertain. Consequently, given the accuracy of $\pm$2% on the relative humidity sensors, it becomes impossible to differentiate between the different walls at this step. To overcome this problem weight samples were installed in the exterior sheathing as described in section 2.4. In this way valuable information about the increased moisture load by natural and forced convection could be obtained (Figure 12). Nevertheless the relative humidity levels at the end of step 4 are in the same range (Figure 11), great differences between the moisture contents are shown in Figure 12.

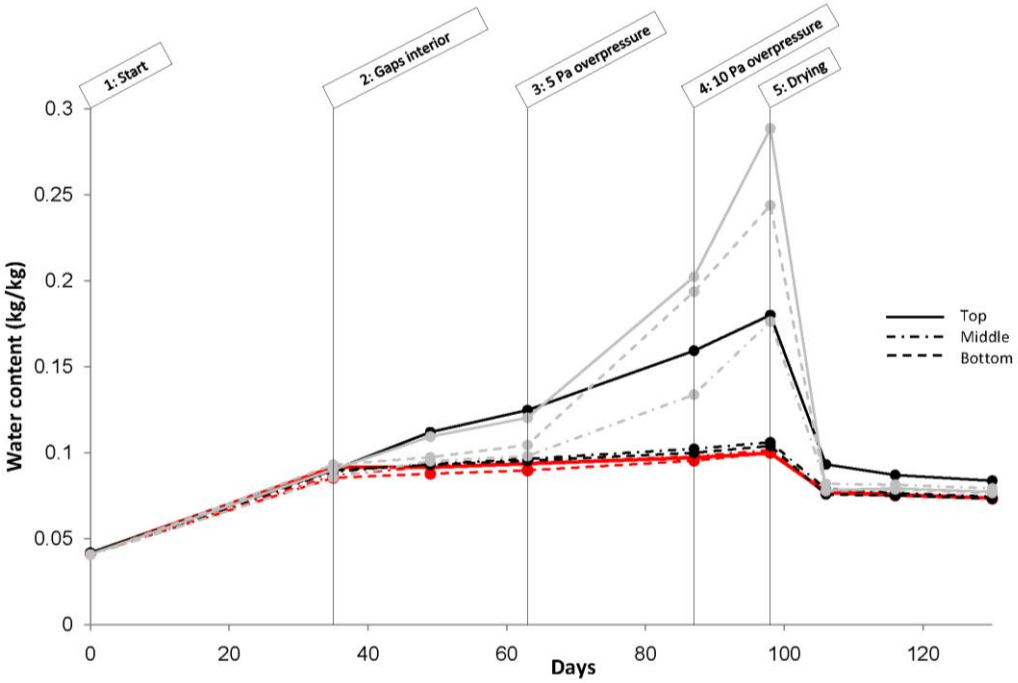

Figure 12. Moisture content evolution of the weight sample in the exterior sheathing: REFERENCE (red), FIBREBOARD 1 (black), FIBREBOARD 2 (grey)

The dots in Figure 12 represent the measured moisture content of the specimens at the top, mid and bottom height. It is important to notice that the measuring points are interconnected with straight lines to clarify the trends. Since the specimens were not weighted during the first step, the initial moisture content is immediately linked to the moisture content at the end of the first step, which explains the discontinuity at the end of this step. During the first stage all weight monster show the same moisture content evolution. However, from the moment the gaps are introduced a significant moisture increase is noticed at the top position. For FIBREBOARD 2 also the moisture content at the bottom and middle position slightly increases indicating the existence of forced convection. Creating in step 3 and 4 a pressure difference across the walls seems to have no influence on the moisture content of FIBREBOARD 1. The moisture content at the upper position continuously increases while the moisture content of the middle and bottom row remains the same as the REFERENCE section. For FIBREBOARD 2 on the other hand – of which the exterior sheathing is twenty times more air open – we can see a clear correlation between the magnitude of the pressure differential and the moisture content of the weight samples at the three heights. As a result of these high moisture contents traces of droplets were found on FIBREBOARD 2 at the end of step 3. After the next step this was already evolved in mould growth at the top and bottom specimens (Figure 13).

Figure 13. Mold growth on weight specimens of FIBREBOARD 2 at the end of step 4 (left to right: top, middle and bottom specimen)

Finally, it is noticed that as a result of the high vapour permeance of all three exterior sheathing materials, the walls can dry out fast.

4. Discussion

As a result of the stricter requirements regarding global building airtightness, the installation of an interior air barrier system becomes more and more time consuming. The introduction presented how recently an increased focus lies upon the continuity of the exterior layer in achieving airtight buildings. This layer shows fewer joints and has consequently a significant potential to minimize the labour cost for airtightness. Although, based on a limited amount of well controlled experiments, the present study shows that this may increase moisture damage risks in light weight construction if the airtightness of the inner barrier can not be guaranteed.

A full scale experiment with three different potential exterior air barrier materials was conducted in laboratory conditions. The results confirm that a sufficiently airtight construction is a prerequisite in obtaining a safe building envelope. To this respect FIBREBOARD 2 (0.1 $m^3/m^2/h/Pa$) obviously fails, resulting in a forced exfiltration flow through the wall, and thus, increased heat losses and very high moisture contents of the exterior sheathing. For FIBREBOARD 1 (0.005 $m^3/m^2/h/Pa$) and FOIL (<0.001 $m^3/m^2/h/Pa$) this effect was limited to a very minimum from which we can conclude that such levels of air permeance are sufficiently low to prevent harmful amounts of forced exfiltration.

On the other hand, the study reveals that even if forced convection is excluded (FIBREBOARD 1 and FOIL), an increased moisture load is introduced by moving the air barrier to the exterior of the building envelope. For both test sections the results indicate that water vapour driven by natural convection enters through the upper gap and deposits at the cold side of the insulation layer. Previous studies [19, 21] showed that the air velocities related to natural convection are too small to influence the overall heat flux of sufficiently dense insulated vertical walls.

However, the current study indicates that such small air velocities can significantly disturb the moisture safety of the wall, if the air barrier is positioned at the outer side of the wall. The danger of this process is its continuity. Driven by the temperature difference across the wall, this convection loop provides a constant moisture supply towards the upper cold side of the structure in winter conditions.

Furthermore, the present study shows the positive impact of using exterior sheathing materials with a thermal resistance and a moisture buffer capacity. The thermal resistance increases the temperature and thus reduces the relative humidity at the cold side of the insulation. The moisture buffer capacity on the other hand has a retarding effect on condensation and can damp out fluctuations of the relative humidity in this way. But although interstitial condensation can be postponed with these materials, the results reveal that this can lead at the same time to more conducive conditions for mould growth at the inside of the exterior air barrier.

Since the measurement aims to produce validation data, the walls were constructed with great care. Consequently, the configuration studied was free from significant air leakages. This of course does not correspond to real building practise and underestimates the moisture load. On the other hand, the walls were exposed to a constant (severe) winter climate which might overestimate the effect of natural convection. Nevertheless, this study gives an important insight in the physical phenomena of light weight walls with an exterior air barrier, it remains difficult to derive its behaviour in real climate conditions.

5. Conclusion

The current paper presents the results of a laboratory experiment to study the hygrothermal behaviour of highly insulated walls with an exterior air barrier. The results show an increased moisture flow at the upper part of the walls driven by buoyancy forces. Consequently, the magnitude of this flow is, apart from the position and size of the gaps, highly depending on the air permeability and the accuracy of the installation of the insulation layer. For the current study (very carefully installed) mineral wool is used which leads to a significant moisture increase. Furthermore, the study shows the preference for hygroscopic exterior sheathing with a thermal resistance to delay condensation conditions.

The present study recognizes the hygrothermal risks of using exterior air barriers in light weight walls. Further tests to investigate the importance of this effect for other insulation materials, such as blown-in cellulose or studying the influence of bad workmanship of the insulation layer would be an added value to this research.

Acknowledgements

Research funded by a Ph.D. grant (grant number 81153) of the Institute for the Promotion of Innovation through Science and Technology in Flanders (IWT-Vlaanderen).

References

[1] Jokisalo J, Kurnitski J, Korpi M, Kalamees T, & Vinha J. Building leakage, infiltration, and energy performance analyses for Finnish detached houses. Building and Environment 2009;44(2):377-387.
[2] Feist W, Schnieders J, Dorer V, Haas A. Re-inventing air heating: Convenient and comfortable within the frame of the Passive House concept. Energy and Buildings 2005;37(11):1186-1203.
[3] The Minergie®-Standard for buildings (2008) http://www.minergie.ch
[4] Janssens A. Reliable control of interstitial condensation in lightweight roof systems. Phd dissertation, K.U.Leuven – Building Physics section. Heverlee; 1998
[5] Desta TZ, Langmans J, Roels S . Experimental data set for validation of heat, air and moisture transport models of building envelopes. Building and Environment 2011:46(5); 1038-1046.
[6] Tenwolde A, Rose WB. Moisture Control Strategies for the Building Envelope . Journal of Building Physics 1996;19(3):206-214
[7] Janssens A, Hens H. Interstitial condensation due to air leakage: a sensitivity analysis. Journal of Thermal Envelope and building science 2003;27(1)15-29.
[8] Janssens A, Hens H, Effects of wind on the transmission heat loss in duo-pitched insulated roofs: A field study. Energy and Buildings 2007;39(9):1047-1054.
[9] Uvsløkk S. The importance of wind barriers for insulated timber frame constructions, Journal of Thermal Insulation and Building Envelopes 1996;20(1)40–62.
[10] Langmans J, Klein R, De Paepe M, Roels S. Potential of wind barriers to assure airtightness of wood-frame low energy constructions. Energy and Buildings 2010;42(12):2376-2385
[11] Aho H, Vinha J, Korpi M. Implementation of airtight constructions and joints in residential buildings. In Proceedings: 8th Symposium on Building Physics in the Nordic Countries. Copenhagen; 2008
[12] Sandberg PI, Sikander E. Airtightness issues in the building process. In Proceedings: 7th Symposium on Building Physics in the Nordic Countries. Reykjavik; 2005, p. 420 427
[13] Sandberg PI, Bankvall C, Sikander E, Wahlgren P, Larsson B, (2007). The effect and cost impact of poor airtightness - information for developers and clients. In Proceedings: Thermal Performance of the Exterior Envelopes of Whole Buildings X International Conference, Clearwater Beach; 2007
[14] Kalamees T. Airtightness and air leakages of new lightweight single-family detached houses in Estonia. Building and Environment 2007;42(6):2369-2377.
[15] http://www.holdtett.no/
[16] Myhre L, Aurlien T. (2005). Measured airtightness in low-energy houses. In Proceedings: 7th Symposium on Building Physics in the Nordic Countries. Reykjavik; 2005, p. 420 427
[17] Holøs, SB, Relander TO. Airtightness Measurements of Wood Frame Low Energy Row Houses. In Proceedings: BEST conference. Portland;2010.
[18] Relander TO, Bauwens G, Roels S, Thue JV, Uvsløkk S. The influence of structural floors on the airtightness of wood-frame houses. Energy and Buildings 2011;43:639-652.
[19] Powell F, Karti M, Tuluca A. Air Movement Influence on the Effective Thermal Resistance of Porous Insulations: A Literature Survey. Journal of Building Physics 1989;12(3): 239-251
[20] Brown WC, Bomberg MT, Ullett JM, Rasmussen J. Measured Thermal Resistance of Frame Walls with Defects in the Installation of Mineral Fibre Insulation. Journal of Building Physics. 1993;16(4): 318-339.
[21] Dyrbøl S, Svendsen S, Elmroth A. Experimental Investigation of the Effect of Natural Convection on Heat Transfer in Mineral Wool. Journal of Building Physics. 2002;26(2):153-164.
[22] Kalamees T, Vinha J. Hygrothermal calculations and laboratory tests on timber-framed wall structures. Building and Environment 2003;38(5):689-697.
[23] Ojanen T, Kumaran K. Effect of Exfiltration on the Hygrothermal Behaviour of a Residential Wall Assembly. Journal of Building Physics 1996;19(3):215-227.
[24] Økland Ø.Convection in highly-insulated building structures. PhD thesis. Norwegian University of Science and Technology.Trondheim;1998.
[25] Riesner K. Natural convection in loose fill insulated walls. Phd thesis. University of Rockstock. Rockstock; 2003 *(in German)*

[26] Riesner K, Hagentoft C-E, Mainka G-W. Condensation risk within loose fill insulation due to natural convection in vertical cavities. In Proceedings: Performance of Exterior Envelopes of Whole Buildings IX International Conference. Clearwater Beach;2004.
[27] International standard. Thermal insulation e Determination of steady- state thermal resistance and related properties - Guarded hot plate apparatus, ISO 8302:1991
[28] Lenardo D. A Method for Evaluating Air Barrier Systems and Materials. Construction. Technical report NRC-CNRC, Montreal; 2009.
[29] Ojanen T, Kohonen R, Kumaran K. Modeling heat, air and moisture transport through building materials and components, in H.R. Trechsel (ed), Moisture control in buildings, Philadelphia;1994
[30] Kumaran K. Material properties - Final report, vol. 3.KU Leuven- Building physics section,Leuven;1996
[31] Kronvall J. Air flows in building components. Phd thesis. Lund institute of technology.Lund;1980
[32] International standard. Hygrothermal performance of building materials and products - Determination of water vapour transmission properties, ISO 12572:2001.
[33] Roels S, Carmeliet J, Hens H, Adan O, Brocken H, Cerny R, et al. A Comparison of Different Techniques to Quantify Moisture Content Profiles in Porous Building Materials. Journal of Thermal Envelope and Building Science. 2004;27(4):261-276.
[34] Langmans J, Klein R, Roels S. Hygrothermal response of highly insulated timber frame walls with an exterior air barrier system: laboratory investigation. In Proceedings: 9th Nordic Symposium on Building Physics. Tampere;2011.